Inorg. Chem. **2003**, *42*, 3788–3795

Cation–Cation Interactions in Neptunyl(V) Compounds: Hydrothermal Preparation and Structural Characterization of $NpO_2(IO_3)$ and α- and β-$AgNpO_2(SeO_3)$

Thomas E. Albrecht-Schmitt,*,† Philip M. Almond, and Richard E. Sykora

Department of Chemistry and Leach Nuclear Science Center, Auburn University, Auburn, Alabama 36849

Received February 4, 2003

The hydrothermal reaction of NpO_2 with IO_3^- in the presence of nitrate results in the formation of $NpO_2(IO_3)$ (**1**). Under similar conditions, NpO_2 reacts with $AgNO_3$ and SeO_2 to yield α-$AgNpO_2(SeO_3)$ (**2**) and β-$AgNpO_2(SeO_3)$ (**3**). The structure of **1** consists of distorted pentagonal bipyramidal Np(V) centers that are bridged by iodate anions. In addition, the oxo atoms of the neptunyl(V) cations coordinate adjacent Np(V) centers creating layers that are linked into a three-dimensional network structure by the iodate anions. The structure is polar owing to the alignment of the stereochemically active lone pair of electrons on the iodate anions along the *c*-axis. α-$AgNpO_2(SeO_3)$ (**2**) forms a layered structure consisting of hexagonal bipyramidal NpO_8 polyhedra that are bound by chelating and bridging selenite anions. The primary and secondary structures of **3** are similar to those of **1**, and neptunyl–neptunyl interactions are partially responsible for the creation of a three-dimensional network structure. However, the selenite anions in **3** are rotated with respect to the iodate anions found in **1**, and the structure is centrosymmetric. The network found in **3** consists of interconnecting, approximately square channels that house the Ag^+ cations. A bond-valance sum parameter of 2.036 Å for Np(V) bound exclusively to oxygen has been developed with $b = 0.37$ Å. Crystallographic data: **1**, orthorhombic, space group $Pna2_1$, $a = 13.816(2)$ Å, $b = 5.8949(8)$ Å, $c = 5.5852(8)$ Å, $Z = 4$; **2**, monoclinic, space group $P2_1/n$, $a = 4.3007(3)$ Å, $b = 9.5003(7)$ Å, $c = 11.5877(9)$ Å, $\beta = 95.855(1)°$, $Z = 4$; **3**, triclinic, space group $P\bar{1}$, $a = 7.1066(6)$ Å, $b = 8.3503(7)$ Å, $c = 8.3554(7)$ Å, $\alpha = 89.349(1)°$, $\beta = 77.034(1)°$, $\gamma = 76.561(1)°$, $Z = 2$.

Introduction

The stabilization of early actinides in the +V and +VI oxidation states is achieved by the formation of approximately linear dioxo cations for which uranyl, UO_2^{2+}, is especially well-known.[1] The oxo atoms of actinyl(VI) cations are typically found to be terminal, but they do participate in hydrogen bonding and long-range ionic interactions with water molecules or additional cations that are crucial to the formation of crystalline structures.[2] $PbUO_2(SeO_3)_2$ illustrates this structural principle quite well because while the oxo atoms of the uranyl cations are utilized in the formation of distorted PbO_5 square pyramids, the Pb−O bonds to these oxo atoms are quite long at 2.683(5) and 2.708(6) Å.[3] The coordination sphere of actinyl(VI) cations is completed by binding up to six additional atoms perpendicular to the AnO_2^{2+} (An = U, Np, Pu) axis leading to the formation of tetragonal bipyramidal, pentagonal bipyramidal, or hexagonal bipyramidal units.[4] It is anticipated that because one direction of connectivity is lost owing to the terminal nature of the actinyl(VI) oxo atoms that the majority of extended structures containing these cations should be layered; this prediction is borne out in a survey of known uranyl(VI) compounds.[4]

In surprising contrast to the coordination chemistry of actinyl(VI) cations, actinyl(V) cations are known to participate in cation−cation interactions (CCIs) whereby the oxo

* To whom correspondence should be addressed. E-mail: albreth@auburn.edu.

† Authors appear in alphabetical order.

(1) Weigel, F. Uranium. In *The Chemistry of the Actinide Elements*, 2nd ed.; Katz, J. J., Seaborg, G. T., Morss, L. R., Eds.; Chapman and Hall: London, 1986; Chapter 5, pp 169−442.

(2) Burns, P. C.; Ewing, R. C.; Hawthorne, F. C. *Can. Mineral.* **1997**, *35*, 1551.

(3) Almond, P. M.; Albrecht-Schmitt, T. E. *Inorg. Chem.* **2002**, *41*, 1177.

(4) Burns, P. C.; Miller, M. L.; Ewing, R. C. *Can. Mineral.* **1996**, *34*, 845.

10.1021/ic034124z CCC: $25.00
Published on Web 05/09/2003

atoms of the AnO_2^+ units coordinate one another. This phenomenon was first recognized by Sullivan and co-workers in 1961, who found complexation of UO_2^{2+} by NpO_2^+ in solution.[5] These interactions have been probed by a variety of spectroscopic techniques including absorption,[5,6] vibrational,[6c,7] Mössbauer,[8] and laser-induced photoacoustic spectroscopy,[9] and large-angle X-ray scattering.[10] The apparent cause of these interactions is a residual negative charge on the oxo atoms of the AnO_2^+ units.[11] In contrast, the oxo atoms of AnO_2^{2+} cations bear some of the positive charge of the cation and are poor donors.[11] CCIs are now known to occur in solution for most combinations of AnO_2^+ (An = U, Np, Pu, Am) with UO_2^{2+},[5−12] NpO_2^+ with NpO_2^+,[7a,10,12b] NpO_2^+ with Al^{3+}, Ga^{3+}, Sc^{3+}, Fe^{3+}, Cu^{2+}, Rh^{3+}, In^{3+}, and BiO^+,[6a,b,7a] NpO_2^+ with VO_2^+ and VO^{2+},[7b] AnO_2^+ with Cr^{3+},[13] and AnO_2^+ (An = Np, Pu) with Th^{4+}.[9]

Despite substantial efforts to address the nature of CCIs in solution, these contacts were unknown in the solid state until 1984 when $[Na_4(NpO_2)_2(C_{12}O_{12})]\cdot 8H_2O$ was shown via single crystal X-ray diffraction to contain a neptunyl(V)−neptunyl(V) dimer.[11] To date, CCIs in the solid state are only known for NpO_2^+−NpO_2^+.[14] This lacuna can be ascribed to the higher stability of Np(V) versus most other An(V) cations, which are subject to disproportion, oxidation, and reduction.[1,15] More recently, neptunyl(V)−neptunyl(V) coordination has been observed in the solid state with a variety of ligands including formates[14,16] and carboxylates,[11] such as $[NpO_2(O_2CH)(H_2O)]$[16] and $[(NpO_2)_2(CH_3COO)_2(H_2O)]\cdot C_2H_3N$,[17] aquo,[18] and dimethyl sulfoxide,[19] and in purely inorganic phases such as $Na_2[(NpO_2)_2(MoO_4)_2(H_2O)]\cdot H_2O$.[20] These CCIs can yield dimers, or lead to the formation of one-, two-, or three-dimensional networks.[16] The donating ability of the oxo atoms of NpO_2^+ has been postulated to be similar to XO_4^{2-} (X = S, Se, Cr, Mo).[21] While it can be argued that most NpO_2^+−NpO_2^+ interactions are supported by additional bridging ligands, the recent report of the structure of $(NpO_2)(CH_3CONH_2)_2(NO_3)$, which contains zigzagging chains formed from the coordination of neptunyl(V) by adjacent neptunyl(V) units, clearly demonstrates that additional bridging ligands are not required.[22]

Compounds containing neptunyl(V)−neptunyl(V) coordination provide a remarkable opportunity to examine the magnetic properties of Np(V) compounds where Np(V)···Np(V) distances can be less than 3.5 Å.[11] While such studies are still quite limited, ferromagnetic ordering has been observed at 12.8 K in $NpO_2(O_2CH)(H_2O)$,[23] and metamagnetic behavior was found in $[(NpO_2)_2(O_2C)_2C_6H_4]\cdot 4H_2O$.[24] There is some controversy over the magnetic behavior of $(NpO_2)_2C_2O_4\cdot 4H_2O$,[25] which was originally interpreted as being metamagnetic, but it may in fact be a ferromagnet.[23] The development of new, well-defined phases containing CCIs provides for additional opportunities to explore the electronic structure of Np(V) compounds as well as an increased understanding of the solid state chemistry of neptunium, which is certainly still unresolved. Herein we report the hydrothermal preparation and structural characterization of the first well-characterized Np(V) iodate, $NpO_2(IO_3)$ (**1**), and the first neptunium selenites, α-$AgNpO_2(SeO_3)$ (**2**) and β-$AgNpO_2(SeO_3)$ (**3**). $NpO_2(IO_3)$ (**1**) and β-$AgNpO_2(SeO_3)$ (**3**) both contain neptunyl(V)−neptunyl(V) interactions. In addition, we have developed the bond-valence sum[26,27] parameter for Np(V) bound to oxygen to aid in oxidation state assignment. While Np(V) iodates, such as $NpO_2IO_3\cdot 0.5KIO_3\cdot 2H_2O$, have been reported, these compounds have been characterized only by elemental analyses and IR spectroscopy.[28]

(5) Sullivan, J. C.; Hindman, J. C.; Zielen, A. J. *J. Am. Chem. Soc.* **1961**, *83*, 3373.

(6) (a) Sullivan, J. C. *J. Am. Chem. Soc.* **1962**, *84*, 4256. (b) Sullivan, J. C. *Inorg. Chem.* **1964**, *3*, 315. (c) Murmann, R. K.; Sullivan, J. C. *Inorg. Chem.* **1967**, *6*, 892. (d) Rykov, A. G.; Frolov, A. A. *Radiokhimiya* **1972**, *14*, 709. (e) Frolov, A. A.; Rykov, A. G. *Radiokhimiya* **1974**, *16*, 556. (f) Rykov, A. G.; Frolov, A. A. *Radiokhimiya* **1975**, *17*, 187. (g) Madic, C.; Guillaume, B.; Morisseau, J. C.; Moulin, J. P. *J. Inorg. Nucl. Chem.* **1979**, *41*, 1027.

(7) (a) Guillaume, B.; Begun, G. M.; Hahn, R. L. *Inorg. Chem.* **1982**, *21*, 1159. (b) Madic, C.; Begun, G. M.; Hobart, D. E.; Hahn, R. L. *Radiochim. Acta* **1983**, *34*, 195. (c) Andreev, G. B.; Budantseva, N. A.; Antipin, M. Yu.; Krot, N. N. *Russ. J. Coord. Chem.* **2002**, *28*, 434. (d) Nakada, M.; Yamashita, T.; Nakamoto, T.; Saeki, M.; Krot, N. N.; Grigor'ev, M. S. *Radiochemistry (Moscow)* **2002**, *44*, 103.

(8) (a) Karraker, D. G.; Stone, J. A. *Inorg. Chem.* **1977**, *16*, 2979. (b) Nectoux, F.; Abazli, H.; Jové, J.; Cousson, A.; Pagès, M.; Gasperin, M.; Choppin, G. *J. Less-Common Met.* **1984**, *97*, 1. (c) Nakada, M.; Nakamoto, T.; Masaki, N. M.; Saeki, M.; Yamashita, T.; Krot, N. N. *Conference Proceedings of ICAME'97, Hyperfine Interactions (C)* **1998**, *3*, 129.

(9) Stoyer, N. J.; Hoffman, D. C.; Silva, R. J. *Radiochim. Acta* **2000**, *88*, 279.

(10) Guillaume, B.; Hahn, R. L.; Narten, A. H. *Inorg. Chem.* **1983**, *22*, 109.

(11) Cousson, A.; Dabos, S.; Abazli, H.; Nectoux, F.; Pagès, M.; Choppin, G. *J. Less-Common Met.* **1984**, *99*, 233.

(12) (a) Newton, T. W.; Baker, F. B. *Inorg. Chem.* **1965**, *4*, 1166. (b) Stout, B. E.; Choppin, G. R.; Nectoux, F.; Pages, M. *Radiochim. Acta* **1993**, *61*, 65. (c) Guillaume, B.; Hobart, D. E.; Bourges, J. Y. *J. Inorg. Nucl. Chem.* **1981**, *43*, 3295.

(13) (a) Newton, T. W.; Burkart, M. J. *Inorg. Chem.* **1971**, *10*, 2323. (b) Ekstrom, A.; Farrar, Y. *Inorg. Chem.* **1972**, *11*, 2610.

(14) (a) Krot, N. N.; Suglobov, D. N. *Radiokhimiya* **1989**, *6*, 1. (b) Krot, N. N.; Suglobov, D. N. *Radiochemistry (Moscow)* **1990**, 619.

(15) (a) Clark, D. L.; Hobart, D. E.; Neu, M. P. *Chem. Rev.* **1995**, *95*, 25. (b) Clark, D. L.; Conradson, S. D.; Ekberg, S. A.; Hess, N. J.; Neu, M. P.; Palmer, P. D.; Runde, W.; Tait, C. D. *J. Am. Chem. Soc.* **1996**, *118*, 2089.

(16) (a) Grigor'ev, M. S.; Yanovskii, A. I.; Struchkov, Yu. T.; Bessonov, A. A.; Afonas'eva, T. V.; Krot, N. N. *Radiokhimiya* **1989**, *31*, 37. (b) Grigor'ev, M. S.; Yanovskii, A. I.; Struchkov, Yu. T.; Bessonov, A. A.; Afonas'eva, T. V.; Krot, N. N. *Radiochemistry (Moscow)* **1990**, 397. (c) Krot, N. N.; Suglobov, D. N. *Radiokhimiya* **1989**, *31*, 1.

(17) Charushnikova, I. A.; Perminov, V. P.; Katser, S. B. *Radiokhimiya* **1995**, *37*, 493.

(18) Grigor'ev, M. S.; Baturin, N. A.; Bessonov, A. A.; Krot, N. N. *Radiokhimiya* **1995**, *37*, 15.

(19) Charushnikova, I. A.; Krot, N. N.; Starikova, Z. A. *Radiokhimiya* **2001**, *43*, 23.

(20) Grigor'ev, M. S.; Baturin, N. A.; Fedoseev, A. M.; Budantseva, N. A. *Russ. J. Coord. Chem.* **1994**, *20*, 523.

(21) Serezhkina, V. N.; Krivopalova, M. A.; Serezhkina, L. B. *Russ. J. Coord. Chem.* **1998**, *24*, 59.

(22) Andreev, G. B.; Budantseva, N. A.; Antipin, M. Yu.; Krot, N. N. *Russ. J. Coord. Chem.* **2002**, *28*, 434.

(23) Nakamoto, T.; Nakada, M.; Nakamura, A.; Haga, Y.; Onuki, Y. *Solid State Commun.* **1999**, *109*, 77.

(24) Nakamoto, T.; Nakada, M.; Nakamura, A. *Solid State Commun.* **2001**, *119*, 523.

(25) Jones, E. R., Jr.; Stone, J. A. *J. Chem. Phys.* **1972**, *56*, 1343.

(26) Brown, I. D.; Altermatt, D. *Acta Crystallogr.* **1985**, *B41*, 244.

(27) Brese, N. E.; O'Keeffe, M. *Acta Crystallogr.* **1991**, *B47*, 192.

(28) (a) Blokhin, V. I.; Bukhtiyarova, T. N.; Krot, N. N.; Gel'man, A. D. *Russ. J. Inorg. Chem.* **1972**, *17*, 1742−1746. (b) Tsivadze, A. Y.; Muchnik, B. I.; Krot, N. N. *Russ. J. Inorg. Chem.* **1972**, *17*, 1746−1749.

Experimental Section

Syntheses. $^{237}NpO_2$ (99.9%, Oak Ridge), $AgNO_3$ (99.9%, Fisher), SeO_2 (99.4%, Alfa Aesar), CsCl (99.9%, Alfa Aesar), HIO_3 (Alfa Aesar, 99.5%), and I_2O_5 (98%, Alfa Aesar) were used as received. Distilled and Millipore filtered water with a resistance of 18.2 MΩ was used in all reactions. Reactions were run in Parr 4749 autoclaves with custom-made 10-mL PTFE liners. Semiquantitative SEM/EDX analyses were performed using a JEOL 840/Link Isis instrument. *^{237}Np ($t_{1/2} = 2.14 \times 10^6$ years) represents a serious health risk owing to its α and γ emission, and especially because of its decay to the short-lived isotope ^{233}Pa ($t_{1/2} = 27.0$ days), which is a potent β and γ emitter.* All studies were conducted in a lab dedicated to studies on transuranium elements. This lab is located in a nuclear science facility and is equipped with a HEPA filtered hood and glovebox that is ported directly into the hood. A series of counters continually monitor radiation levels in the lab. The lab is licensed by the state of Alabama (a NRC compliant state) and Auburn University's Radiation Safety Office. All experiments were carried out with approved safety operating procedures. All free-flowing solids are worked with in the glovebox and products are only examined when coated with either water or Krytox oil and water. There are some limitations in accurately determining yield because this requires weighing dry solids, which possess a health risk as well as manipulation difficulties. Therefore, the yields had to be estimated. For $NpO_2(IO_3)$ (**1**), the estimated yield is nearly quantitative because it is the only solid that forms and no Np remains in solution. The yields of α-$AgNpO_2(SeO_3)$ (**2**) and β-$AgNpO_2(SeO_3)$ (**3**) are estimated on the basis of counting the number of crystals of each compound and making measurements of their approximate size. Then, the yield of each compound could be estimated from the density calculated from the crystal structure. From these measurements, we estimate the yield at close to 80-(10)% (40% of each).

$NpO_2(IO_3)$ (1). NpO_2 (11 mg, 0.041 mmol), $AgNO_3$ (6.7 mg, 0.039 mmol), and I_2O_5 (13 mg, 0.039 mmol) were loaded in a 10-mL PTFE-lined autoclave followed by the addition of 0.75 mL of water. The autoclave was sealed and placed in a preheated furnace for 3 days at 180 °C. The box furnace was cooled at 9 °C/h to 23 °C. The product consisted of a colorless solution over square tablets of **1** that had a green coloration. The crystals were generally quite small and had a maximum dimension of approximately 0.060 mm. The majority of the mother liquor was removed from the crystals, and additional water was added to keep the crystals under solution. A few crystals of **1** were selected for X-ray diffraction studies and EDX measurements. These crystals were then coated with Krytox oil. The presence of Np and I in the crystals was confirmed by EDX analysis; Ag was not detected. Standards are not available for Np on this instrument, and the results were not quantified.

α-$AgNpO_2(SeO_3)$ (2) and β-$AgNpO_2(SeO_3)$ (3). NpO_2 (10.0 mg, 0.037 mmol), $AgNO_3$ (13.4 mg, 0.079 mmol), and SeO_2 (8.8 mg, 0.097 mmol) were loaded in a 10-mL PTFE-lined autoclave followed by the addition of 0.75 mL of water. The autoclave was sealed and placed in a preheated furnace for 3 days at 180 °C. The box furnace was cooled at 9 °C/h to 23 °C. The products consisted of a pale green solution over an approximately 1:1 mixture of clusters of pale green acicular crystals of **2** and brown blocks of **3**. The needles of **2** were on the order of 0.1 mm in length. Twinned crystals of **3** were as large as 0.3 mm, but single crystals were typically under 0.1 mm on a side. A few crystals of **2** and **3** were selected for X-ray diffraction studies and EDX measurements. These crystals were then coated with Krytox oil. EDX analysis for **2** and **3** provided a Ag/Se ratio of 1:1. Np energy peaks were observed but could not be quantified owing to instrument limitations.

Crystallographic Studies. Crystals of **1**−**3** suitable for single crystal X-ray diffraction experiments were selected using a CCD camera located in a HEPA filtered hood. Mounted crystals were secured on goniometer heads, cooled to −80 °C with an Oxford Cryostat, and optically aligned on a Bruker SMART APEX CCD X-ray diffractometer using a digital camera. A rotation photo was taken for each crystal, and a preliminary unit cell was determined from three sets of 30 frames with 20 s exposure times using SMART. The unit cell of **3** could conceivably be represented in a *C*-centered monoclinic setting. However, the α angle is 89.68(1)° in the monoclinic setting, and the structure factor intensities are inconsistent with monoclinic symmetry. Furthermore, the structure cannot be solved in a *C*-centered monoclinic space group. Twinning was not observed when tested for by using RLATT or GEMINI. Missed symmetry in the triclinic solution was also checked for using PLATON;[29] none was suggested. The structure is triclinic. All intensity measurements were performed using graphite monochromated Mo Kα radiation from a sealed tube with a monocapillary collimator. For all compounds, the intensities of reflections of a sphere were collected by a combination of three sets of exposures. Each set had a different ϕ angle for the crystal, and each exposure covered a range of 0.3° in ω. A total of 1800 frames were collected with an exposure time per frame of 30 s for **1**−**3**.

For **1**−**3**, determination of integral intensities and global cell refinement were performed with the Bruker SAINT (v 6.02) software package using a narrow-frame integration algorithm. A face-indexed analytical absorption correction was initially applied using XPREP.[30] Individual shells of unmerged data were corrected analytically and exported in the same format. These files were subsequently treated with a semiempirical absorption correction by SADABS[31] with a $\mu \cdot t$ parameter of 0.[32] The program suite SHELXTL (v 5.1) was used for space group determination (XPREP), direct methods structure solution (XS), and least-squares refinement (XL).[30] The final refinements included anisotropic displacement parameters for all atoms and a secondary extinction parameter. All of the structures proved to be of high quality. Some crystallographic details are listed in Table 1. Additional details can be found in the Supporting Information. Bond lengths and angles are listed in Tables 2−4.

Bond-Valence Calculations. Data used to calculate the bond-valence parameter for Np(V) were obtained from comprehensive searches for crystal structure reports using the Cambridge Crystallographic Structural Database (CCSD), the Inorganic Crystal Structure Database (ICSD), SciFinder Scholar, Science Citation Index, and manual searches. Four compounds recently prepared by our group were also included in the calculation. Constraints were not placed on the *R* factors of reported structures, which were generally quite good. Disordered structures were excluded from the calculation. Only structures that contained Np(V) sites bonded exclusively to oxygen atoms were used in our calculations. A total of 57 crystallographically independent Np sites from 41 different crystal structures were used to calculate the bond-valence parameter.

(29) Spek, A. L. *Acta Crystallogr.* **1990**, *A46*, C34.
(30) Sheldrick, G. M. *SHELXTL PC, Version 5.0, An Integrated System for Solving, Refining, and Displaying Crystal Structures from Diffraction Data*; Siemens Analytical X-ray Instruments, Inc.: Madison, WI, 1994.
(31) *SADABS*. Program for absorption correction using SMART CCD based on the method of Blessing: Blessing, R. H. *Acta Crystallogr.* **1995**, *A51*, 33.
(32) Huang, F. Q.; Ibers, J. A. *Inorg. Chem.* **2001**, *40*, 2602.

Table 1. Crystallographic Data for $NpO_2(IO_3)$ (**1**), α-$AgNpO_2(SeO_3)$ (**2**), and β-$AgNpO_2(SeO_3)$ (**3**)

	$NpO_2(IO_3)$	α-$AgNpO_2(SeO_3)$	β-$AgNpO_2(SeO_3)$
color	green	pale green	dark brown
formula mass (amu)	443.90	503.83	503.83
space group	$Pna2_1$ (No. 33)	$P2_1/n$ (No. 14)	$P\bar{1}$ (No. 2)
a (Å)	13.816(2)	4.3007(3)	7.1066(6)
b (Å)	5.8949(8)	9.5003(7)	8.3503(7)
c (Å)	5.5852(8)	11.5877(9)	8.3554(7)
α (deg)	90	90	89.349(1)
β (deg)	90	95.855(1)	77.034(1)
γ (deg)	90	90	76.561(1)
V (Å^3)	454.9(1)	470.98(6)	469.52(7)
Z	4	4	2
T (°C)	−80	−80	−80
λ (Å)	0.71073	0.71073	0.71073
ρ_{calcd} (g cm^{-3})	6.482	7.105	7.128
μ(Mo Kα) (cm^{-1})	295.39	337.45	338.49
$R(F)$ for $F_o^2 > 2\sigma(F_o^2)$[a]	0.0197	0.0222	0.0226
$R_w(F_o^2)$[b]	0.0432	0.0534	0.0542

[a] $R(F) = \{\sum||F_o| - |F_c||\}/\{\sum|F_o|\}$. [b] $R_w(F_o^2) = [\{\sum[w(F_o^2 - F_c^2)^2]\}/\{\sum wF_o^4\}]^{1/2}$.

Table 2. Selected Bond Distances (Å) and Angles (deg) for $NpO_2(IO_3)$ (**1**)

Distances (Å)			
Np(1)−O(1)	2.404(5)	Np(1)−O(5)	1.843(6) (NpO_2^+)
Np(1)−O(2)′	2.422(6)	Np(1)−O(5)′	2.475(5)
Np(1)−O(3)′	2.506(6)	I(1)−O(1)	1.793(5)
Np(1)−O(4)	1.891(6) (NpO_2^+)	I(1)−O(2)	1.804(6)
Np(1)−O(4)′	2.475(5)	I(1)−O(3)	1.812(5)

Angles (deg)			
O(4)−Np(1)−O(5)	175.5(2) (NpO_2^+)	O(1)−I(1)−O(2)	97.7(3)
Np(1)−O(4)−Np(1)′	144.9(3)	O(1)−I(1)−O(3)	97.4(3)
Np(1)−O(5)−Np(1)′	157.8(3)	O(2)−I(1)−O(3)	98.7(3)

Table 3. Selected Bond Distances (Å) and Angles (deg) for α-$AgNpO_2(SeO_3)$ (**2**)

Distances (Å)			
Np(1)−O(1)	2.516(4)	Np(1)−O(5)	1.822(4) (NpO_2^+)
Np(1)−O(1)′	2.440(4)	Ag(1)−O(4)	2.288(5)
Np(1)−O(2)′	2.445(4)	Ag(1)−O(5)′	2.577(5)
Np(1)−O(2)′	2.519(4)	Ag(1)−O(5)′	2.587(5)
Np(1)−O(3)	2.695(4)	Se(1)−O(1)	1.679(5)
Np(1)−O(3)′	2.705(4)	Se(1)−O(2)	1.664(4)
Np(1)−O(4)	1.837(5) (NpO_2^+)	Se(1)−O(3)	1.702(4)

Angles (deg)			
O(4)−Np(1)−O(5)	179.3(2) (NpO_2^+)	O(1)−Se(1)−O(2)	101.9(4)
O(4)−Ag(1)−O(5)′	115.6(2)	O(1)−Se(1)−O(3)	94.8(2)
O(4)−Ag(1)−O(5)′	90.9(2)	O(2)−Se(1)−O(3)	95.0(2)
O(5)′−Ag(1)−O(5)′	112.8(2)		

We employed the following exponential to calculate the bond-valence parameter, R_{ij}, for Np(V) and oxygen.[26,27]

$$R_{ij} = b \ln[V_i / \sum_j \exp(-d_{ij}/b)]$$

The valence, V_i, was fixed at 5, and the sums of valence contributions from all inner-sphere ligands bonded to Np were conducted using calculated bond lengths, d_{ij}, and a b value of 0.37 Å.[26,27] The bond-valence parameter was calculated for each Np(V) site, and the values were averaged to obtain a final mean R_{ij}.

Results and Discussion

Syntheses. The hydrothermal reaction of NpO_2 with $AgNO_3$ and I_2O_5 at 180 °C for 3 days results in the formation of $NpO_2(IO_3)$ (**1**). We observed that the use of a solid Np(IV) starting material allows for the isolation of a Np(V) compound that did not form when Np(V) stock solutions were used, and instead, only Np(VI) solids were isolated.[33] α-$AgNpO_2(SeO_3)$ (**2**) and β-$AgNpO_2(SeO_3)$ (**3**) simultaneously form under mild hydrothermal conditions from the reaction of NpO_2 with $AgNO_3$ and SeO_2. This reaction is quite spectacular because it results in the formation of beautiful clusters of pale green needles of **2** and rich brown blocks of **3** in an approximate ratio of 1:1. Despite their dissimilar habits and coloration, which reflects their markedly different structures, they have identical composition. Some Np(V) remains in solution during the preparation of **2** and **3** as evidenced by the pale green mother liquor.

Table 4. Selected Bond Distances (Å) and Angles (deg) for β-$AgNpO_2(SeO_3)$ (**3**)

Distances (Å)			
Np(1)−O(1)	2.412(4)	Ag(1)−O(1)′	2.588(5)
Np(1)−O(3)′	2.432(4)	Ag(1)−O(3)′	2.491(5)
Np(1)−O(5)′	2.401(4)	Ag(1)−O(4)′	2.350(4)
Np(1)−O(7)	1.881(4) (NpO_2^+)	Ag(1)−O(6)′	2.419(5)
Np(1)−O(8)	1.867(4) (NpO_2^+)	Ag(2)−O(2)′	2.560(5)
Np(1)−O(9)′	2.463(4)	Ag(2)−O(2)′	2.347(5)
Np(1)−O(10)′	2.449(4)	Ag(2)−O(6)′	2.435(5)
Np(2)−O(2)′	2.377(4)	Ag(2)−O(7)	2.540(5)
Np(2)−O(4)	2.394(4)	Se(1)−O(1)	1.697(4)
Np(2)−O(6)′	2.450(4)	Se(1)−O(2)	1.721(4)
Np(2)−O(7)′	2.488(4)	Se(1)−O(3)	1.697(4)
Np(2)−O(8)	2.418(5)	Se(2)−O(4)	1.704(4)
Np(2)−O(9)	1.853(4) (NpO_2^+)	Se(2)−O(5)	1.673(4)
Np(2)−O(10)	1.876(4) (NpO_2^+)	Se(2)−O(6)	1.712(5)

Angles (deg)			
O(7)−Np(1)−O(8)	178.0(2)	O(1)−Se(1)−O(2)	99.2(2)
Np(1)−O(7)−Np(2)′	153.0(2)	O(1)−Se(1)−O(3)	99.9(2)
Np(1)′−O(9)−Np(2)	153.4(2)	O(2)−Se(1)−O(3)	98.5(2)
O(9)−Np(2)−O(10)	177.4(2)	O(4)−Se(2)−O(5)	100.7(2)
Np(1)−O(8)−Np(2)	166.7(3)	O(4)−Se(2)−O(6)	97.1(2)
Np(1)′−O(10)−Np(2)	164.3(2)	O(5)−Se(2)−O(6)	102.5(2)

Bond-Valence Sums for Np(V). Bond-valence sums for all transuranium elements except Cf were unavailable at the time of this research.[27] The oxidation state of actinyl(V) and actinyl(VI) compounds can usually be inferred from the An═O bond lengths and/or the AnO_2^{n+} (n = 1 or 2) stretching frequencies.[2,4,15] However, this distance shows some variation with changes in the coordination number and the identity of additional ligands. Tetragonal bipyramidal $An(VI)O_6$ units are particularly problematic because the An═O bond lengths can be long enough in some compounds to speculate an An(V) species.[2] Therefore, it is useful to look at the total contribution of all ligands to the oxidation state of the actinide in question. Vibrational spectroscopy of Np(V) compounds that also contain iodate and selenite is problematic because the vibrational modes of the anions overlap with the NpO_2^+ modes.[34,35]

(33) Bean, A. C.; Albrecht-Schmitt, T. E.; Scott, B. L.; Runde, W. *Inorg. Chem.*, submitted.
(34) (a) Pracht, G.; Lange, N.; Lutz, H. D. *Thermochim. Acta* **1997**, *293*, 13. (b) Pracht, G.; Nagel, R.; Suchanek, E.; Lange, N.; Lutz, H. D. *Z. Anorg. Allg. Chem.* **1998**, *624*, 1355. (c) Schellenschläger, V.; Pracht, G.; Lutz, H. D. *J. Raman Spectrosc.* **2001**, *32*, 373. (d) Peter, S.; Pracht, G.; Lange, N.; Lutz, H. D. *Z. Anorg. Allg. Chem.* **2000**, *626*, 208.
(35) Nakamoto, K. *Infrared and Raman Spectra of Inorganic and Coordination Compounds*, 5th ed.; Wiley-Interscience: New York, 1997.

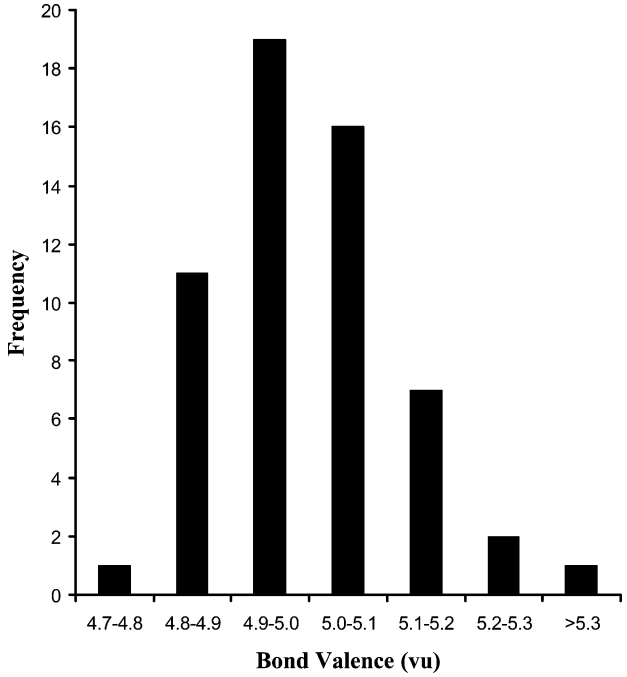

Figure 1. Distribution of bond-valence sums, R_{ij}, for Np(V) compounds calculated using $d_{ij} = 2.036$ Å and $b = 0.37$ Å.

The bond-valence parameter, R_{ij}, calculated for Np(V) with $b = 0.37$ Å was 2.036 Å, and the distribution of bond-valence sums calculated using this parameter is shown in Figure 1. The bond-valence parameter was calculated without discrimination on the basis of coordination number as done by Burns et al. for U(VI),[2] although it would be desirable to do so. However, there are only eight examples of hexagonal bipyramidal Np(V) and only two examples of tetragonal bipyramidal coordination for Np(V). In contrast, analysis of single crystal X-ray structures revealed 47 Np(V) sites with pentagonal bipyramidal coordination. If only the seven-coordinate Np(V) sites are used to calculate the bond-valence parameter, a value of 2.035 Å is found. The compounds possessing $NpO_2^+ - NpO_2^+$ bonds do not show any peculiarities in their bond-valence sums. The bond-valence parameters for the other common oxidation states of neptunium, namely IV, VI, and VII, have not been rigorously investigated.

Structures. $NpO_2(IO_3)$ (1). The structure of **1** consists of neptunyl(V) cations that are linked to one another by both $NpO_2^+ - NpO_2^+$ bonds and by bridging iodate anions creating the pentagonal bipyramidal NpO_7 building unit shown in Figure 2a. Oxygen atoms from the iodate anions occupy three of the equatorial sites in the NpO_7 units. The remaining two sites are filled by oxo atoms from neighboring neptunyl(V) cations. Both oxo atoms of the neptunyl(V) units are involved in coordinating adjacent Np(V) centers, leading to the creation of a two-dimensional neptunium oxide sheet similar to the one found in $[NpO_2(O_2CH)(H_2O)]$,[16] as shown in Figure 3. The iodate anions link the neptunyl(V) sheets together into a three-dimensional network that is depicted in Figure 4. This network is polar owing to the alignment of the stereochemically active lone pair of electrons on the iodate anions along the *c*-axis, which is consistent with the polar space group, $Pna2_1$, found for **1**. While noncentrosymmetric structures are relatively common when stereoactive lone pairs of electrons are present,[36] this trend is typically

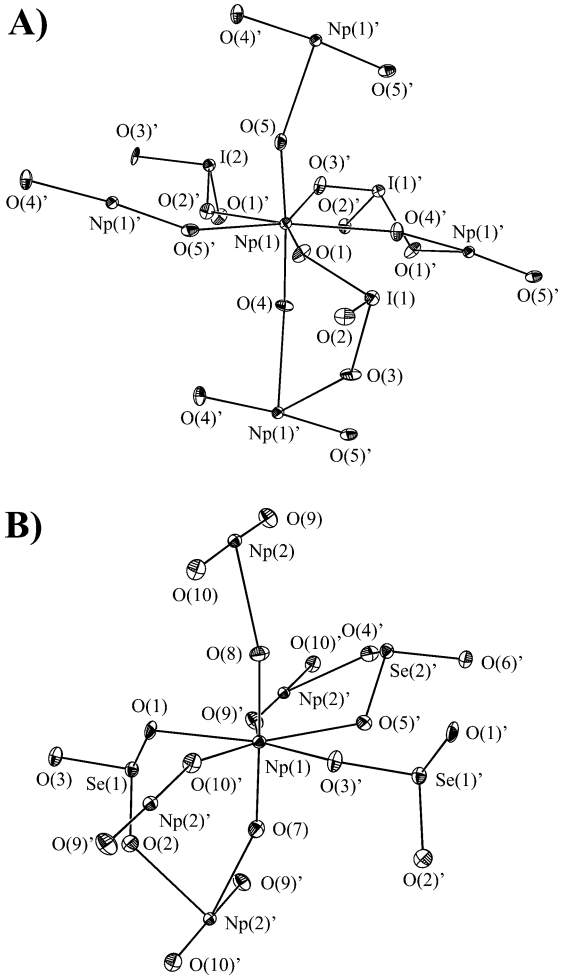

Figure 2. Depiction of the local coordination environment of the Np(V) centers in (a) $NpO_2(IO_3)$ (**1**) and (b) β-$AgNpO_2(SeO_3)$ (**3**) showing the neptunyl(V)−neptunyl(V) bonds. 50% probability ellipsoids are shown.

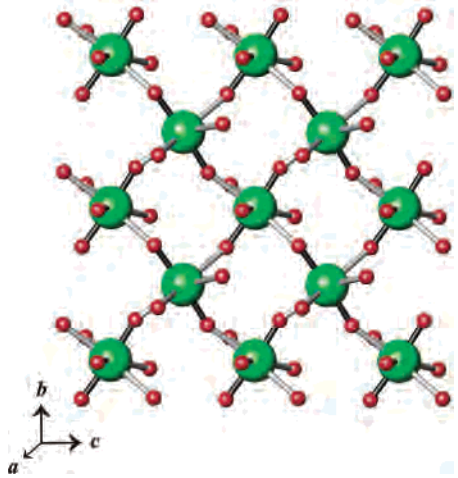

Figure 3. View down the *a*-axis showing part of a two-dimensional neptunium oxide sheet in $NpO_2(IO_3)$ (**1**) formed by the coordination of Np(V) centers with oxo atoms from neighboring neptunyl(V) cations. The NpO_2^+ cation bonds are shown in black for emphasis. Similar layers are also found in β-$AgNpO_2(SeO_3)$ (**3**). The neptunium atoms are shown in green and oxygen in red.

(36) Halasyamani, P. S.; Poeppelmeier, K. R. *Chem. Mater.* **1998**, *10*, 2753.

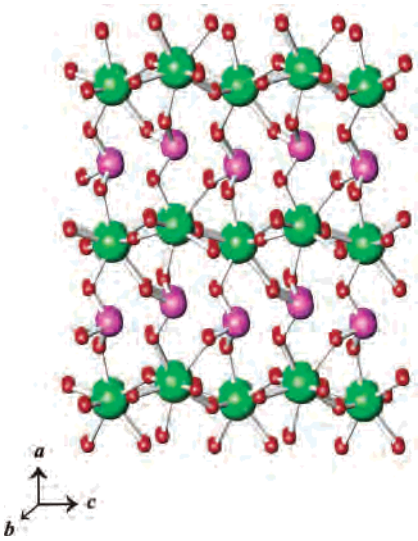

Figure 4. Depiction of part of the polar, three-dimensional network structure of $NpO_2(IO_3)$ (**1**) showing the alignment of the stereochemically active lone pair of electrons on the iodate anions along the *c*-axis. Green = Np, purple = I, and red = O.

not observed in compounds with actinyl(VI) units because these linear cations can be placed on, or be related by, inversion centers.[3,37,38] The O═Np═O bond angle of 175.5(2)° is more perturbed from linearity than normally found when CCIs are not present in Np(V) compounds. It may well be that the substantial perturbation of the NpO_2^+ unit in **1** allows for the formation of a polar structure.

Another important difference between the coordination environment of the neptunyl(V) cations versus neptunyl(VI) cations is that the five oxygen atoms in the equatorial plane of the NpO_7 polyhedra in **1** deviate from planarity by 0.12 Å, which is larger than is typically found in An(VI) compounds. The Np═O bond lengths of 1.843(6) and 1.891(6) Å are consistent with Np(V)[15] and are substantially longer than the Np(VI)═O bonds found in $NpO_2(IO_3)_2(H_2O)$ and $NpO_2(IO_3)_2{\cdot}H_2O$, which have an average distance of 1.763(8) Å.[33] Furthermore, the bond-valence sum[26,27] of the Np atom in **1** was determined to be 4.90 using parameters described in this work, which is consistent with Np(V). The Np—O bonds derived from the CCIs at 2.475(5) Å are similar in length with the Np—O from the iodate anions which range from 2.404(5) to 2.506(6) Å.

α-AgNpO$_2$(SeO$_3$) (2). The layered structure of **2** is assembled from NpO_2^+ cations that are bound by two chelating and two bridging SeO_3^{2-} anions yielding hexagonal bipyramidal NpO_8 polyhedra. A thermal ellipsoid plot of a

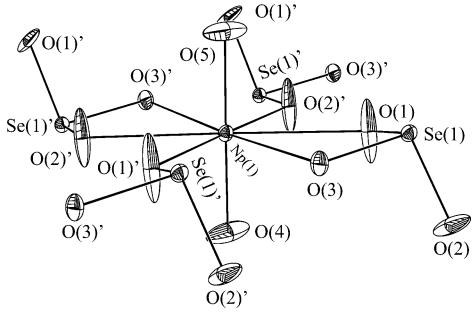

Figure 5. View of a $[NpO_2(SeO_3)_4]$ unit in α-$AgNpO_2(SeO_3)$ (**2**) containing a NpO_8 hexagonal bipyramid formed from the binding of a NpO_2^+ cation by two chelating and two bridging SeO_3^{2-} anions. 50% probability ellipsoids are shown.

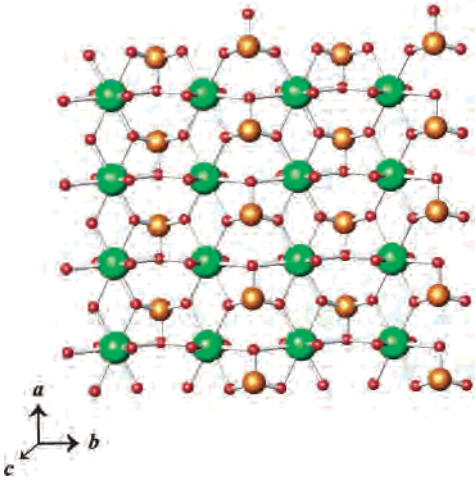

Figure 6. Illustration of the $^2_\infty[NpO_2(SeO_3)]^{1-}$ layers formed from NpO_8 hexagonal bipyramids and SeO_3^{2-} anions in α-$AgNpO_2(SeO_3)$ (**2**). Green = Np, orange = Se, and red = O.

$NpO_2(SeO_3)_4$ unit is shown in Figure 5. From this view, it is evident that there is disorder in some of the equatorial oxygen positions, and perhaps in the neptunyl oxo positions. However, the disorder is not of sufficient magnitude to warrant splitting the current positions of the atoms. We have carefully examined the X-ray data for **2** to check if the thermal ellipsoid elongation is an artifact of absorption or incorrect space group assignment, but no such errors were evident. It is apparent from the structure of **1** that the equatorial atoms around neptunyl(V) are not always as planar as is typically found in uranyl(VI) compounds. This disorder is probably a consequence of this. The NpO_8 units are joined by virtue of the fact that all of the oxygen atoms of the SeO_3^{2-} anions are μ_3 and, therefore, bridge two neptunyl(V) cations. The resultant layers, shown in Figure 6, extend in the [*ab*] plane and are separated by Ag^+ cations. Eight-coordinate Np(V) and Np(VI) are much less common than seven-coordinate NpO_7 pentagonal bipyramids; this is a structural feature that parallels uranyl crystal chemistry.[2,4] While this structure type is superficially similar to a number of layered uranyl selenite phases, such as $Ag_2(UO_2)(SeO_3)_2$,[3] none of these contain UO_8 polyhedra, and none contain selenite anions in this ligating mode.[3,4,37,38] The Ag^+ are not behaving as pseudo-alkali metals in this compound and instead form short to intermediate Ag—O bonds ranging from 2.288(5) to 2.587(5) Å. These bonds are not formed

(37) (a) Almond, P. M.; Albrecht-Schmitt, T. E. *Inorg. Chem.* **2002**, *41*, 5495. (b) Almond, P. M.; Peper, S. M.; Bakker, E.; Albrecht-Schmitt, T. E. *J. Solid State Chem.* **2002**, *168*, 358. (c) Bean, A. C.; Albrecht-Schmitt, T. E. *J. Solid State Chem.* **2001**, *161*, 416. (d) Bean, A. C.; Campana, C. F.; Kwon, O.; Albrecht-Schmitt, T. E. *J. Am. Chem. Soc.* **2001**, *123*, 8806. (e) Bean, A. C.; Ruf, M.; Albrecht-Schmitt, T. E. *Inorg. Chem.* **2001**, *40*, 3959. (f) Bean, A. C.; Peper, S. M.; Albrecht-Schmitt, T. E. *Chem. Mater.* **2001**, *13*, 1266. (g) Sykora, R. E.; Wells, D. M.; Albrecht-Schmitt, T. E. *Inorg. Chem.* **2002**, *41*, 2304. (h) Sykora, R. E.; McDaniel, S. M.; Wells, D. M.; Albrecht-Schmitt, T. E. *Inorg. Chem.* **2002**, *41*, 5126. (i) Bean, A. C.; Xu, Y.; Danis, J. A.; Albrecht-Schmitt, T. E.; Runde, W. *Inorg. Chem.* **2002**, *41*, 6775.
(38) Almond, P. M.; McKee, M. L.; Albrecht-Schmitt, T. E. *Angew. Chem., Int. Ed.* **2002**, *114*, 3576.

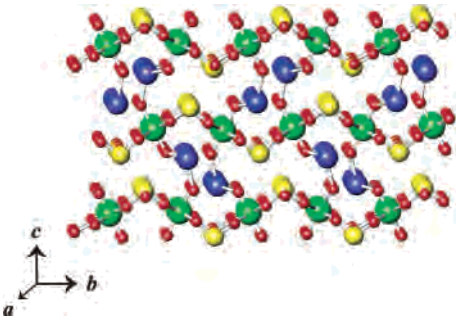

Figure 7. $^{2}_{\infty}[NpO_2(SeO_3)]^{1-}$ layers in α-$AgNpO_2(SeO_3)$ (**2**) are connected via Ag^+ cations that are coordinated by oxo atoms from neptunyl(V) cations. Green = Np, blue = Ag, orange = Se, and red = O.

with the selenite anions because all of the oxygen atoms from these anions are utilized in the formation of the $^{2}_{\infty}[NpO_2(SeO_3)]^{1-}$ layers, but rather, they are formed with the oxo atoms of the NpO_2^+ cations. Figure 7 shows a view down the *a*-axis that illustrates the coordination of the Ag^+ cations by neptunyl(V).

The Np═O bond distances of 1.822(4) and 1.837(5) Å are significantly shorter than those found in **1** but are still within normal limits for Np═O bonds in NpO_2^+ cations.[11−22] By looking at the total contribution of all inner-sphere ligands to the charge, i.e., the bond-valence sum, we find that the Np center in **2** has a valence of 5.04, which is consistent with Np(V). The NpO_2^+ bond angle of 179.3(2)° deviates little from linearity. The Se═O bond distances are 1.664(4), 1.679(5), and 1.702(4) Å and show no evidence of protonation as was found in $A[(UO_2)(HSeO_3)(SeO_3)]$ (A = K, Rb, Cs, Tl) where the Se−(OH) bond distances average 1.764(4) Å.[3] Therefore, there is little ambiguity in the oxidation state of **2**.

***β*-$AgNpO_2(SeO_3)$ (3).** The basic repeating unit in **3** is quite similar to that observed in **1** and is shown for comparison in Figure 2b. Therefore, it is not surprising that neptunium oxide layers formed from NpO_2^+−NpO_2^+ bonds found in **1** also occur in **3**. However, the change from IO_3^- anions to SeO_3^{2-} anions requires the incorporation of additional cations for charge neutrality, and the Ag^+ cations play this role in **3**. A depiction of part of the structure of **3** viewed down the *a*-axis is shown in Figure 8. As can be seen from this figure, the structure is three-dimensional, and the neptunyl oxide layers are linked together by selenite anions. The selenite anions are rotated with respect to the iodate anions in **1**, and the structure of **3** is centrosymmetric. When the structure is viewed down this axis, it becomes apparent that there are three types of channels running through the neptunyl selenite lattice. Two of these have oxygen atoms from the selenite anions and the oxo atoms from the neptunyl(V) cations directed into the channels that are used to bind the Ag^+ cations. The third type of channel has the stereochemically active lone pair of the selenite anions directed into it. Given the strongly nonbonding nature of these lone pairs, it is not surprising to find these channels vacant of Ag^+ cations.

There are two crystallographically unique Np atoms in **3**, as well as two unique selenite anions, and two unique silver atoms. We discussed earlier that the unit cell of this

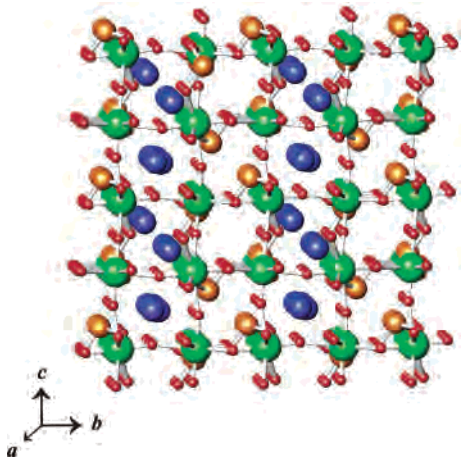

Figure 8. View down the *a*-axis of the three-dimensional structure of *β*-$AgNpO_2(SeO_3)$ (**3**). Green = Np, blue = Ag, orange = Se, and red = O.

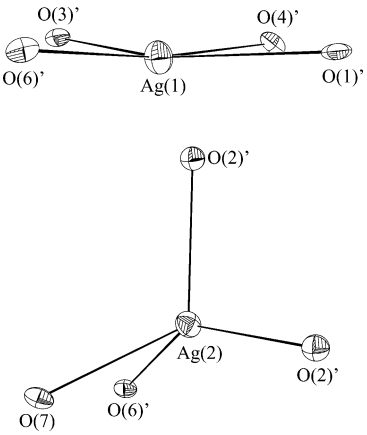

Figure 9. Depiction of the distorted square planar and tetrahedral coordination environments for Ag(1) and Ag(2), respectively, in *β*-$AgNpO_2(SeO_3)$ (**3**). 50% probability ellipsoids are shown.

compound could conceivably be represented in a *C*-centered monoclinic setting, and the observation of a doubled unit leads to further suspicion that symmetry was missed. However, while the two Np centers and the two selenite anions have similar bond distances and angles, the two Ag^+ cations have markedly dissimilar environments. The geometry of Ag(1) is approximately square planar and deviates from planarity by 0.054 Å with Ag−O bond distances that range from 2.350(4) to 2.588(5) Å. The angles around the Ag(1) center range from 75.9(2)° to 99.8(2)° whereas the environment of Ag(2) is a distorted tetrahedron with Ag−O bond distances ranging from 2.347(5) to 2.560(5) Å and O−Ag−O angles spanning 97.4(1)−140.7(2)°. The coordination environments of Ag(1) and Ag(2) are shown in Figure 9. It is likely that these atoms are responsible for the symmetry reduction. The NpO_2^+ bonds and angles of 1.867(4) and 1.881(4) Å and 178.0(2)° for Np(1) and 1.876(4) and 1.853(4) Å and 177.4(2)° for Np(2) are consistent with Np(V), and these two Np centers have bond-valence sums of 4.82 and 4.93 (vide infra). The selenite anions show no indication of being protonated as indicated by Se═O bonds of 1.697(4) (×2) and 1.721(4) Å to Se(1), and 1.673(4), 1.704(4), and 1.712(5) Å to Se(2).

Conclusion

The question that remains largely unanswered at the end of this study is why is **2** green and **3** brown if they both contain the same elements in the same oxidation states? Green coloration is expected from Np(V) compounds, including those with cation−cation interactions, and a survey indicates that they are all green unless another color producing moiety is present. Therefore, the brown color of **3** is anomalous. A possible explanation for the color of **3** came from the structure of $Np(NpO_2)_2(SeO_3)_3$, which was recently prepared by us.[39] $Np(NpO_2)_2(SeO_3)_3$ contains crystallographically distinct Np(IV) and Np(V) sites and also possesses brown color. Here, the brown color is consistent with mixed valence and the presence of Np(IV). A second review of the bond-valence sums for the Np centers in **3** leads us to speculate that the brown color of **3** may be the result of partial reduction of Np in this compound giving rise to Np(IV) and hence brown coloration. Spectroscopic studies on **3** and $Np(NpO_2)_2(SeO_3)_3$ will aid in addressing this issue and will be performed once appropriate instrumentation is available in our transuranium research facility.

(39) Albrecht-Schmitt, T. E.; Almond, P. M.; Sykora, R. E. *Inorg. Chem.*, in preparation.

Acknowledgment. This work was supported by the U.S. Department of Energy, Office of Basic Energy Sciences, Heavy Elements Program (Grant DE-FG02-01ER15187). We thank J. W. King, C. H. Ray, Jr., J. L. Schnurrenberger, and M. B. Schnurrenberger of the Radiation Safety Office at Auburn University for facilitating the establishment of our transuranium research center, and J. D. Perez for providing suitable laboratory space in the Leach Nuclear Science Center. We also thank technical staff members at ORNL, ANL, and LANL for encouragement in the establishment of this lab. We also thank W. Runde for helpful comments made during a preview of this manuscript.

Supporting Information Available: X-ray crystallographic files for $NpO_2(IO_3)$ (**1**), α-$AgNpO_2(SeO_3)$ (**2**), and β-$AgNpO_2(SeO_3)$ (**3**) in CIF format. This material is available free of charge via the Internet at http://pubs.acs.org.

IC034124Z